NG2 expressed by macrophages and oligodendrocyte precursor cells is dispensable in experimental autoimmune encephalomyelitis

Moransard, M ; Dann, A ; Staszewski, O ; Fontana, A ; Prinz, M ; Suter, T

Abstract: Increased expression of the chondroitin proteoglycan NG2 is a prominent feature in central nervous system injury with unknown cellular source and biological relevance. Here, we describe the first detailed analysis of experimental autoimmune encephalomyelitis in NG2 knockout mice and NG2 knockout bone marrow chimeras. We show that both macrophages and oligodendrocyte progenitor cells express and secrete NG2 in response to transforming growth factor- . A subpopulation of macrophages expresses NG2 within leucocyte infiltrates in the central nervous system, but only oligodendrocyte progenitor cells contribute to NG2 accumulation. Notably, NG2 plays no role in experimental autoimmune encephalomyelitis initiation, progression or recuperation. In concurrence, the immune response is unaltered in NG2-deficient mice as are the extent of central nervous system damage and degree of remyelination.

DOI: https://doi.org/10.1093/brain/awr070

NG2 expressed by macrophages and oligodendrocyte precursor cells is dispensable in Experimental Autoimmune Encephalomyelitis

Running title: **NG2 expression by macrophages in EAE**

Martijn Moransard[1], Angela Dann[2], Ori Staszewski[2], Adriano Fontana[1], Marco Prinz[2,3], and Tobias Suter[1,3]

[1] Clinical Immunology, University Hospital Zurich, Häldeliweg 4, CH-8044 Zürich, Switzerland

[2] Department of Neuropathology, University of Freiburg, Breisacherstrasse 64, D-79106 Freiburg, Germany

[3] These authors contributed equally to this work

Correspondence should be addressed to M.M. (mmoransard@mac.com)

Total number of words in the text: 6354

ABSTRACT

Increased expression of the chondroitin proteoglycan NG2 is a prominent feature in CNS injury with unknown cellular source and biological relevance. Here, we describe the first detailed analysis of experimental autoimmune encephalomyelitis in NG2ko mice and NG2ko bone marrow chimeras. We show that both macrophages and oligodendrocyte progenitors cells express and shed NG2 in response to TGFβ. A subpopulation of macrophages expresses NG2 within leukocyte infiltrates in the CNS, but only oligodendrocyte progenitor cells contribute to NG2 accumulation. Notably, NG2 plays no role in experimental autoimmune encephalomyelitis initiation, progression or recuperation. In concurrence, the immune response is unaltered in NG2 deficient mice as are the extent of CNS damage and degree of remyelination.

Key words: Multiple sclerosis, glial scar, macrophage, oligodendrocyte progenitor, TGFβ

Introduction

The glial scar is considered a major obstacle in effective recovery of the CNS from insult. Virtual all CNS injuries, including the autoimmune disease Multiple Sclerosis (MS), trigger rapid activation of astrocytes, microglia, macrophages and oligodendrocyte progenitor cells (OPCs) (Alonso, 2005, Fawcett and Asher, 1999), which in turn deposit chondroitin sulfate proteoglycans (CSPGs) (Dou and Levine, 1994, Laabs *et al.* , 2007, Tang *et al.* , 2003). The high molecular weight chondroitin proteoglycan NG2 (CSPG-4) is a prominent component of the glial scar (Tan *et al.* , 2005, Tang *et al.* , 2003) and is considered a major obstacle for axon regeneration, remyelination and CNS recovery (Chen *et al.* , 2002, de Castro *et al.* , 2005, Dou and Levine, 1994, Fawcett and Asher, 1999, Laabs *et al.* , 2007, Larsen *et al.* , 2003, Morgenstern *et al.* , 2002, Tan *et al.* , 2005, Tan *et al.* , 2006, Tang *et al.* , 2003), although this view is now being questioned (de Castro *et al.* , 2005, Hossain-Ibrahim *et al.* , 2007 Sep 27, Tan *et al.* , 2006, Ughrin *et al.* , 2003).

Although the rapid accumulation of NG2 is a common feature of damage to the CNS, the biological role of NG2 in CNS injury is still a conundrum. The short intracellular domain of NG2 binds various signaling molecules that may link NG2 to synapses and the cytoskeleton. The large extracellular domain (290 kDa) contains several disulfide bonds, N-glycosylation sites and a single chondroitin chain and binds a wide array of proteins, including receptors, growth factors, extracellular matrix components, and proteases indicating that NG2 may regulate diverse cellular processes (Nishiyama *et al.* , 2009, Stallcup, 2002, Trotter *et al.* , 2010 May). Importantly, the extracellular domain of NG2 can be cleaved off and incorporated into the extracellular matrix (Asher *et al.* , 2005, Nishiyama *et al.* , 1995). The high concentration of proteases and large numbers of NG2 expressing cells at sites of inflammation in the CNS may

explain the high amount of NG2 in the glial scar. The biological function of NG2 shedding in response to CNS injury remains to be addressed.

Surprisingly, the cellular source of NG2 in areas of CNS damage has become a matter of debate. Although OPCs are generally considered responsible for NG2 accumulation (NG2 is a marker for these cells (Nishiyama *et al.* , 2009, Trotter *et al.* , 2010 May)) recent reports indicate that activated microglia and CNS-infiltrating macrophages may also express NG2 after CNS injury (Bu *et al.* , 2001, Fiedorowicz *et al.* , 2008, Jones *et al.* , 2002, Matsumoto *et al.* , 2008, Smirkin *et al.* , 2009 Mar, Yokoyama *et al.* , 2006, Zhu *et al.*). Blood-derived monocytes/macrophages and microglia play pivotal roles in CNS injury and can cause extensive CNS damage including axonopathy and demyelination, events that trigger substantial OPC activation and glial scar formation (Alonso, 2005, Di Bello *et al.* , 1999, Foote and Blakemore, 2005, Mildner *et al.* , 2009, Reynolds *et al.* , 2002, Rhodes *et al.* , 2006). Importantly, NG2 may mediate the inflammatory response of activated microglia (Gao *et al.* , 2010). However the signals triggering NG2 expression in macrophages and microglia are currently unknown and whether these cells do contribute to NG2 accumulation - and their large numbers at sites of inflammation and in the glial scar support such a notion – has not been addressed yet.

In this study we have investigated the cellular source(s) of deposited NG2, the signals triggering NG2 expression and its function in MOG-induced experimental autoimmune encephalomyelitis (EAE), the murine model system for MS. We show that TGFβ up regulates NG2 expression and secretion by OPCs and macrophages and demonstrate that NG2 is redundant in EAE progression, recruitment of leukocytes into the CNS, neuronal damage, demyelination and, importantly, remyelination. Finally, we prove that blood-derived macrophages express NG2 in the CNS during

EAE but do not contribute to the accumulation of NG2 at sites of inflammation. Our data excludes a prominent role for NG2 in immune regulation and regeneration in autoimmune inflammation of the CNS.

Results

NG2 protein accumulates at sites of infiltrating leukocytes in EAE.

In the injured CNS, NG2 protein levels are often elevated at sites of tissue damage and/or inflammation and increased NG2 levels remain associated with the glial scar (Alonso, 2005, Fawcett and Asher, 1999, Levine, 1994, Morgenstern *et al.* , 2002, Tan *et al.* , 2005, Tan *et al.* , 2006). However, in EAE and MS, changes in NG2 levels have been less well described (Di Bello *et al.* , 1999, Reynolds *et al.* , 2002). Examination of NG2 and cytokine mRNA expression by quantitative RT-PCR in the spinal cord at different EAE disease stages showed that at peak disease on day 18 post-immunization (p.i.) (average score 2.78±0.15) NG2 mRNA levels are significantly elevated and remain elevated in the remission phase (rem.; day 43 p.i., average score 2.13±0.07) (Fig. 1A). Notably, the NG2 expression profile correlates well with the expression of TGFβ in the spinal cord, with high expression maintained in the remission phase (Fig. 1A). In contrast mRNA expression levels of IL-2, IL-6, IL-10, TNFα, and IFNγ subsided after the peak phase (Fig. 1A).

Since NG2 exists in both cell-bound and secreted forms (Asher *et al.* , 2005, Nishiyama *et al.* , 1995, Stallcup, 2002), we examined the expression of both soluble and detergent-extracted NG2 protein in spinal cord at different EAE stages by Western blot (Fig. 1B). Both the 300-kDa cell-bound and 290-kDa shed forms of NG2 are significantly elevated during EAE. The highest amount of detergent-extracted NG2 is detected at the peak phase whereas soluble NG2 increased over the course of the disease (Fig. 1B and C).

We investigated by immunohistochemistry if the increase in NG2 protein was restricted to sites of leukocyte infiltration in the spinal cord (Fig. 1D). In the spinal cord of healthy mice (naïve), NG2 is expressed by pericytes associated with blood

vessels, meningeal cells and OPCs (insert shows the typical stellar appearance of OPCs). NG2 expression typical for the meninges (arrow) and satellite cells of the dorsal root ganglia (arrow head) are illustrated in the remission panel (rem.). At peak disease (peak), NG2-immunoreactivity is clearly elevated within and around the borders of the area occupied by infiltrating leukocytes (outlined area). Importantly, within and in close proximity of these sites of leukocyte infiltration, $Olig2^{+}$ OPCs are abundantly present (Supplementary Fig. 3). Note that within infiltrates some areas are completely devoid of NG2-immunoreactivity, probably a sign of extensive tissue damage. The insert illustrates that NG2 is no longer restricted to stellar OPCs but now has a rather diffuse distribution, which is maintained at the remission stage of EAE (rem.). In contrast, in the normal appearing spinal cord at remission (rem. n.a. Sp.C.), distribution of NG2 is indistinguishable from its distribution in healthy mice. Thus both cell-bound and secreted NG2 are up regulated in the spinal cord during EAE and accumulate at sites of leukocyte infiltration.

TGFβ increases NG2 expression and secretion by macrophages and OPCs.

During EAE the CNS is subjected to a steep increase in the concentration of disease-mediating cytokines (Fig. 1A) that could potentially trigger NG2 accumulation by increasing OPC numbers and/or NG2 expression by OPCs. In addition to OPCs, both macrophages and the CNS-resident microglia are potential producers of NG2 (Bu *et al.* , 2001, Fiedorowicz *et al.* , 2008, Jones *et al.* , 2002, Matsumoto *et al.* , 2008, Smirkin *et al.* , 2009 Mar, Yokoyama *et al.* , 2006, Zhu *et al.* , 2010 Mar 31).

We treated bone marrow-derived macrophages and the OPC cell line OLIneu with a variety of cytokines with known roles in EAE, followed by quantitative RT-PCR analysis. Notably, only TGFβ increases expression of NG2 mRNA in both OLIneu

and macrophages (Fig. 2A). In addition IL-6 increased NG2 expression in OLIneu to a similar extent. Subsequent ^{3}H-thymidine incorporation assays indicated that the TGFβ-induced increase in NG2 mRNA in OLIneu is not due to enhanced proliferation (Supplementary Fig. 1). To test if primary OPCs are capable of secreting NG2 and if secreted and/or cell-bound NG2 protein levels are altered by TGFβ, OPC-conditioned media and cell lysates were analyzed by Western blotting (Fig. 2B). TGFβ-treatment of primary OPCs demonstrated that both secreted and cell-bound NG2 amounts increase after 48 hrs. A time course of TGFβ-treatment of OLIneu confirmed these results (Supplementary Fig. 2). Collectively these data show that TGFβ treatment of OPCs induces an increase in cell-bound and secreted NG2 without influencing cell proliferation.

To investigate if macrophages and/or microglia express NG2 protein and possibly secrete NG2 in response to cytokines we treated bone-marrow derived macrophages and the microglial cell line BV2 (Bocchini *et al.* , 1992) with IL-10, TNFα, IFNγ or TGFβ and analyzed their conditioned media and cell lysates by Western blotting. Although untreated macrophages express a small amount of NG2, TGFβ triggers a significant increase in both cell-bound and secreted NG2 (Fig. 2C and D). In contrast, untreated microglia do not express NG2 and TGFβ induced expression of a small amount of cell-bound, but not secreted, NG2 (Fig. 2E). Notably, a comparative Western blot showed that the amount of cell-bound NG2 expressed by microglia is negligible and barely visible compared to the amount produced by either macrophages or OPCs, with the latter producing the highest amount of cell-bound NG2 (Fig. 2F).

Subsequent immunocytochemical analysis (Fig. 2G) showed that OLIneu cells are always $NG2^{+}$ and TGFβ treatment elicits a modest increase in NG2 immunoreactivity. Untreated macrophages are primarily $NG2^{-}$ although occasionally a $NG2^{+}$ cell is

detected. TGFβ treatment triggers a substantial increase in the number of $NG2^+$ macrophages but the intensity of NG2-immunoreactivity varies between cells. Notably, NG2 immunoreactivity was never observed in microglia after any of the treatments. In summary, these data indicate that both macrophages and OPCs up regulate NG2 expression and secretion in response to TGFβ whereas microglia only produce cell-bound NG2 at low levels in response to TGFβ but do not secrete NG2.

NG2 is not required in EAE.

The TGFβ-induced increase in NG2 expression in OPCs and macrophages, which may underlie the accumulation of NG2 at sites of leukocyte infiltration, is likely to be an important response of the CNS to injury, however its function is currently unclear. Therefore, we subjected NG2-deficient (NG2ko) mice (de Castro *et al.* , 2005, Grako *et al.* , 1999, Kucharova and Stallcup, 2010 Mar 10) and littermate control (WT) mice to EAE and followed disease progression (Fig. 3A) and weight loss (Fig. 3B). The absence of NG2 has no significant effect on EAE onset, disease severity or the extent or rate of recovery.

To investigate if the lack of NG2 influences demyelination, neuronal damage and/or astrocyte activation, histology on thoracic spinal cord cross-sections was performed (remission stage) (Fig. 3C). Quantitation of luxol fast blue (LFB) staining revealed that the extent of demyelination is similar in NG2ko and WT mice (Fig. 3D). Also the number of APP positive deposits, indicative of damaged neurons, and GFAP positive astrocytes are comparable in WT and NG2ko animals.

The expression of NG2 by macrophages *in vitro* and the accumulation of NG2 at sites of leukocyte infiltration suggested that NG2 might modulate the inflammatory response in EAE. Therefore different leukocyte subsets were monitored during the

course of EAE in the CNS, spleen and inguinal lymph nodes by histology and flow cytometry but were not found to differ between NG2ko and WT mice (Fig. 3C-E; spleen and lymph node data not shown). Specifically, histology showed that at remission (d29) infiltrating T-cells (CD3), B-cells (B220), and macrophages (Mac-3) are present in comparable numbers in the CNS of WT and NG2ko mice (Fig. 3C and D). In agreement, flow cytometric analysis at remission did not reveal differences in any of the leukocyte populations tested, including T-cells, granulocytes, different dendritic cell types, microglia, and importantly, blood-derived macrophages (Fig. 3E, CNS).

Since NG2 is prominently accumulated within and around areas of leukocyte infiltration, we assessed whether the size and location of the infiltrates within the thoracic and lumbar spinal cord (lumbar not shown) are altered in NG2ko mice during the peak phase by immunohistochemistry (Fig. 3F). Investigation of the distribution of macrophages/activated microglia (CD11b & F4/80) indicates that cell number, total area covered by the cells and penetration of the cells into the spinal cord in relation to the meninges are comparable in WT and NG2ko mice. Note though the quite prominent overlap in macrophage distribution (CD11b & F4/80) and NG2 immunoreactivity in WT mice.

Finally, because remyelination may be inhibited by NG2 accumulation (Larsen *et al.* , 2003) or delayed by NG2-deficiency (Kucharova and Stallcup, 2010 Mar 10), we determined the extent and quality of remyelination by electron microscopy at d40 p.i. and in healthy control animals of each genotype (Fig. 4A - E). Quantitation of the percentage of myelinated axons, axon diameter, myelin thickness and G-ratio indicates that axon integrity and remyelination are comparable between healthy WT and healthy NG2ko mice and at d40 p.i. between both genotypes. As expected though,

myelination is reduced in d40 p.i. animals of both genotypes compared to myelination in healthy controls. The similar increase in the G-ratio at d40 p.i. strongly suggests that initial demyelinated was extensive in the experimental groups. The comparable G-ratios between WT and NG2ko animals at d40 p.i., however, show that remyelination occurs with similar efficiency in both genotypes. In summary, NG2 deficiency has no influence on EAE disease outcome, the extent of CNS tissue damage, cellular inflammatory response, demyelination or remyelination.

CNS resident cells are responsible for NG2 accumulation within and around infiltrates.

Although our *in vitro* data indicates that both OPCs and macrophages up regulate and secrete NG2 in response to TGFβ, it still remains to be established if these cell types actually contribute to NG2 accumulation at sites of leukocyte infiltration in the CNS during EAE. Furthermore, it is possible that NG2 expression by OPCs or macrophages may have different or even opposite functions in CNS inflammation. To resolve these issues the following bone marrow chimeras were created: WT mice containing NG2ko bone marrow (KO→WT) resulting in mice with NG2 deficiency only in the immune compartment, NG2ko mice containing WT bone marrow (WT→KO) creating mice that express NG2 only in bone marrow-derived leukocytes, and wild type mice containing WT bone marrow (WT→WT) as controls. We subjected these different groups to EAE and, in good agreement with the previous results (Fig. 3), weight-loss, onset, severity and progression of EAE were all comparable in the different chimeras (Fig. 5A and B) indicating that CNS- and leukocyte-derived NG2 do not have opposing or compensatory roles.

To determine the relative contribution of CNS-resident and CNS-infiltrating cells to the increase in NG2 in the spinal cord during EAE, the expression of soluble and detergent-extracted NG2 was examined by Western blot (remission) (Fig. 5C and D). Both 300-kDa cell-bound and 290-kDa shed NG2 are significantly elevated in WT→WT and KO→WT chimeras compared to NG2 levels in naïve WT mice. Notably, the amounts of soluble and cell-bound NG2 do not differ significantly between these two chimeras. In sharp contrast, in spinal cord lysates from WT→KO chimeras cell-bound and soluble NG2 were never detected by Western blotting.

Analysis of thoracic spinal cord for NG2 and CD11b immunoreactivity by confocal microscopy showed that the location and number of infiltrating $CD11b^+$ leukocytes do not vary significantly between the different chimeras (Fig. 5D). However, the distribution of NG2 is strikingly different. WT→WT chimeras show NG2 accumulated within and around the area covered by the infiltrating cells and co-localization of CD11b and NG2-immunoreactivity can on occasion be observed (inserts). Importantly, the distribution and accumulation of NG2 in the KO→WT chimeras is comparable and also in these chimeras occasional CD11b and NG2 co-localization can be seen, albeit significantly less frequently. In contrast, increased NG2 expression and accumulation at sites of leukocyte infiltration are clearly abolished in WT→KO chimeras. Within the infiltrate occasionally NG2-expressing cells (insert), which are also dimly $CD11b^+$, can be observed. NG2-expressing cells were never detected outside infiltrates in WT→KO chimeras. Notably though, the majority of $CD11b^+$ leukocytes do not express NG2. On average, 3 to 4 $NG2^+$ cells are present within an infiltrate, which are all dimly $CD11b^+$.

Taken together, these results indicate that, although some blood-borne $NG2^+$ /$CD11b^+$ macrophages are present in the CNS during EAE, CNS resident cells are responsible for the increase in NG2 and its accumulation at sites of leukocyte infiltration.

Discussion

OPCs are the source of accumulated NG2 at sites of leukocyte infiltration in EAE.

The prominent increase in NG2 mRNA and protein in the CNS during the course of EAE can in theory be derived from various cellular sources. In particular OPCs, CNS-infiltrating macrophages and CNS-resident microglia are likely to express or up-regulate NG2 during EAE. Indeed, our *in vitro* data shows that all three cell-types are able to express or up-regulate NG2 expression in response to TGFβ but not in response to various other cytokines that have been shown to play a role in EAE. In addition, of the various cytokine expression profiles we tested only expression of TGFβ correlated well with the expression of NG2 over the course of EAE, suggesting that TGFβ signaling may trigger increased NG2 expression in EAE.

To determine which of the aforementioned cell types contribute to NG2 accumulation in the CNS we induced EAE in various NG2ko bone marrow chimeras. Our data shows that large amounts of NG2 are only accumulated in and around areas of leukocyte infiltration if the recipient mice have a wild-type background (KO→WT and WT→WT chimeras) showing that increases in NG2 are derived from a CNS-resident cell type. Although it is possible that the lack of NG2 on peripheral cells, in particular leukocytes, may hamper CNS infiltration, which in turn could explain the lack of NG2 accumulation in the CNS, our immunohistochemical and flow cytometric data (latter not shown for chimeras) showing a comparable degree of cellular infiltration and lesion size argues against this possibility.

Notably, in WT→KO chimeras, in which NG2 is expressed by bone marrow-derived cells (leukocytes) and not by CNS resident cells, only a small amount of NG2 is present in the CNS at peak EAE. Notably, lesion size and leukocyte infiltration into the CNS are comparable to control EAE-diseased mice. This small amount of NG2 is

expressed solely by not yet fully characterized, but bone marrow-derived, $CD11b^+$ amoeboid-shaped cells. The actual amount of NG2 expressed by these cells in the spinal cord of WT→KO chimeras was too low to be detected by western blot. Thus, NG2 found in and around lesion sites in the CNS during the course of EAE is derived from CNS resident cells rather than from leukocytes infiltrating from the periphery into the CNS, practically ruling out blood-borne macrophages as a major source of NG2 in EAE. These data agree with observations by Rhodes *et al.* showing that NG2 increases before $ED1^+$ macrophages infiltrate into LPS injected rat brains (Rhodes *et al.* , 2006).

Arguably, microglia as one of the potential brain resident sources of NG2 are unlikely to contribute to NG2 accumulation during EAE because of two observations. Firstly, even in the presence of TGFβ, the amount of cell-bound NG2 expressed by microglia *in vitro* is negligible, and shed NG2 is not produced at all by microglia, which is in good agreement with microarray data from our lab indicating that NG2 is not expressed by TGFβ-treated primary microglia (Paglinawan *et al.* , 2003). Secondly, in KO→WT chimeric mice, in which NG2 is only expressed by CNS resident cells and not by leukocytes, only sporadic co-localization between NG2 and the microglial/macrophage marker CD11b is observed despite leukocyte infiltration into the CNS and lesion sizes being indistinguishable from control EAE-diseased mice. Although the latter observation suggest that some microglia may express NG2 during EAE, the amount produced by these cells cannot account for the large NG2 deposits observed in and around infiltrates.

Taken together, our data rather suggests that OPCs responding to TGFβ are the source of accumulated NG2 in areas of CNS injury because $Olig2^+$ OPCs are prominently present in and around infiltrates (Supplementary Fig. 3) and, *in vitro*, OPCs produce

significantly larger amounts of both cell-bound and soluble NG2 in response to TGFβ than macrophages and microglia. Our data is in accord with the observation that a single injection of TGFβ into the rat basal ganglia elicits OPC activation and increased NG2 immunoreactivity (Rhodes *et al.* , 2006). Functionally, TGFβ may induce a reactive phenotype in OPCs with a concomitant increase in NG2 expression, which may precede differentiation into oligodendrocytes and subsequent remyelination (McKinnon *et al.* , 1993).

Notably, the localization of accumulated NG2 at sites of leukocyte infiltration appears rather diffuse and has a lack of distinct cellar structure indicating that NG2 is partly shed and incorporated into the extracellular matrix, which is confirmed by our Western blot data showing significant increases in both saline-soluble and detergent-extracted NG2. Interestingly, the shedding of NG2 appears to be a common response in CNS injury because increases in both shed and cell-bound NG2 have also been described in knife lesions of rat cerebral cortex (Asher *et al.* , 2005). Although the functional significance of shed NG2 is currently unclear, the ability of the shed domain to bind various growth factors and extracellular matrix components suggests that it may function as a molecular "sink", sequestering growth factors thereby limiting cell migration and/or proliferation. However, our data clearly shows that NG2 does not limit leukocyte proliferation and migration within the CNS or impairs clinical recovery in EAE. Notably, the latter observation, the presence of Olig2+ OPCs in and around areas of leukocyte infiltration (Supplementary Fig. 3), and the comparable extent of remyelination between NG2ko and WT mice at the late remission phase also imply that OPC migration, proliferation and differentiation are neither majorly hampered by NG2 accumulation nor by NG2 deficiency.

Unfortunately the diffuse appearance of the NG2 staining in infiltrates also makes it impossible to determine the number of $NG2^+$ OPCs and $NG2^+/CD11b^+$ macrophages within these infiltrates by immunohistochemistry. Additional attempts to quantify these cell populations by flow cytometric analysis were also unsuccessful due to the lack of anti-NG2 antibodies that work in FACS.

$NG2^+$ macrophages in EAE.

Many recent reports have suggested that macrophage- and/or microglia-like $NG2^+$ cells accumulate in the CNS after a variety of insults (Bu *et al.* , 2001, Fiedorowicz *et al.* , 2008, Gao *et al.* , 2010, Hampton *et al.* , 2004, Jones *et al.* , 2002, Matsumoto *et al.* , 2008, Rezajooi *et al.* , 2004, Smirkin *et al.* , 2009 Mar, Wu *et al.* , 2010, Yokoyama *et al.* , 2006, Zhu *et al.* , 2010 Mar 31), despite this large body of data, claims made in earlier studies indicating that $NG2^+$ cells are quite distinct from macrophages and microglia still cast some doubts on the existence of $NG2^+$ macrophages (Dawson *et al.* , 2000, Di Bello *et al.* , 1999, Levine, 1994, Nishiyama *et al.* , 1997). Some of these original studies have argued that the occasional $NG2^+$ microglia/macrophage engulfed or phagocytized rather than synthesized NG2 (Levine, 1994, Nishiyama *et al.* , 1997). Our data shows that the existence of a macrophage-like $NG2^+$ cell in the CNS after insult can no longer be logically disputed. $NG2^+/CD11b^+$ cells are clearly present in leukocyte infiltrates in the spinal cord of EAE diseased chimeras in which the CNS is NG2 deficient (WT→KO chimeras). Furthermore, our *in vitro* data demonstrates that NG2 expression can be induced in bone marrow-derived macrophages ($CD11b^+$ and $F4/80^+$ expression of these cells shown in (Moransard *et al.* , 2010 Apr)). Concurrent with our data is the observation of $NG2^+/F4/80^+$ macrophages outside the CNS (Tigges *et al.* , 2008). The

quantitative appreciation of the NG2 expression by macrophages in EAE lesions is difficult due to the fact that the usually strongly $CD11b^+$ cuffs of the macrophages are "flooded" by soluble NG2. Interestingly, our observations in the NG2 chimeras show that $NG2^+/CD11b^+$ cells constitute a remarkably small part of all the $CD11b^+$ cells present in infiltrates in the CNS indicating that these cells form a distinct subpopulation. This small number of $NG2^+/CD11b^+$ cells probably explains why these cells have evaded conclusive identification for so long.

Notably, the studies mentioned above have used slightly different panels of antibodies and as a consequence it is not quite clear if we have identified the same cell population or if there are different subpopulations of $NG2^+$ macrophage-like cells. The $NG2^+$ cells we observe in the WT→KO chimeras are dimly $CD11b^+$ and a proportion of these cells also express the DC marker CD11c (data not shown), which would correspond well with the $NG2^+/OX42^+$ cells identified by a number of groups (Bu *et al.* , 2001, Fiedorowicz *et al.* , 2008, Gao *et al.* , 2010, Hampton *et al.* , 2004, Wu *et al.* , 2010, Zhu *et al.* , 2010 Mar 31), which may be myeloid or inflammatory dendritic cells (Hesske *et al.* , 2010 Jun, Mildner *et al.* , 2009).

NG2 plays no role in EAE.

Despite the fact that a number of reports have identified immune cells that express NG2 (Bu *et al.* , 2001, Fiedorowicz *et al.* , 2008, Gao *et al.* , 2010, Hampton *et al.* , 2004, Jones *et al.* , 2002, Matsumoto *et al.* , 2008, Rezajooi *et al.* , 2004, Smirkin *et al.* , 2009 Mar, Wu *et al.* , 2010, Yokoyama *et al.* , 2006, Zhu *et al.* , 2010 Mar 31) and increases in NG2 appear to be a pronounced injury response both in the CNS and PNS (Asher *et al.* , 2005, Di Bello *et al.* , 1999, Hossain-Ibrahim *et al.* , 2007 Sep 27, Jones *et al.* , 2002, Levine, 1994, Moon and Fawcett, 2001, Morgenstern *et al.* , 2002,

Nishiyama *et al.* , 1997, Reynolds *et al.* , 2002, Rezajooi *et al.* , 2004, Tan *et al.* , 2005, Tang *et al.* , 2003), in depth studies investigating the role of NG2 in the immune response have been lacking. Only two recent studies have tried to address the role of $NG2^+$ macrophage/microglia-like cells in CNS inflammation directly. Data by Goa *et al.* indicate that NG2 mediates the induction of iNOS and inflammatory cytokine but not chemokine expression in LPS-activated microglia (Gao *et al.* , 2010). A report by Smirkin *et al.* identifies several neuro-protective factors expressed by $Iba1^+/NG2^+$ macrophage-like cells and suggests that these cells may ameliorate ischemic brain damage (Smirkin *et al.* , 2009 Mar). However, our data demonstrates that NG2 deficiency has no significant effect on EAE progression, leukocytes extravasation or migration within the CNS, demyelination or the extent of neuronal damage, indicating that NG2 does not play an important role in macrophage/microglia function in autoimmunity.

In addition, NG2 accumulation has no effect on remyelination. Although we did not address axon outgrowth directly, the comparably clinical recovery and extent of neuronal damage and de- and remyelination at remission in NG2ko mice and WT littermates indicate that NG2 is not a major inhibitory or stimulatory factor in axon outgrowth, which is in good agreement with the lack of improvement in axon outgrowth observed in the NG2ko mouse after spinal cord injury (de Castro *et al.* , 2005, Hossain-Ibrahim *et al.* , 2007 Sep 27).

In summary, the TGFβ-induced expression of NG2 in macrophages *in vitro* and expression of NG2 by a small population of blood-borne macrophages in the CNS of EAE diseased mice are indicative of a novel, potentially anti-inflammatory, macrophage subpopulation. However, neither CNS-derived nor peripheral macrophage expressed NG2 plays a role in the course of CNS autoimmunity. Finally,

although we have established here that shed and accumulated NG2 is derived from CNS resident OPCs, the biological role of this rather prominent response of the CNS to injury remains an open question.

Materials and Methods

Mice

Seven to eight week old C57Bl/6 female mice were purchased from Harlan (the Netherlands). NG2 knockout mice were a kind gift from Prof. William B. Stallcup, Burnham Institute for Medical Research, La Jolla, CA, USA and backcrossed to C57Bl/6 background for 9 generations.

To generate bone marrow-chimeras, mice were lethally irradiated with a split-dose of 1000 rad. Donor animals were euthanized with CO_2 and bones (fore- and hind legs, hips) were flushed with sterile PBS to obtain bone marrow stem cells. In total, 5×10^6 total bone marrow cells were injected i.v. per mouse. To prevent bacterial infection 1% Neomycin (Sigma) was added for 2 weeks to the drinking water. After 6 weeks, prior to MOG immunization, reconstitution was verified by flow cytometry with anti-CD45.1 and anti-CD45.2 (BD PharMingen) on circulating leukocytes isolated from blood samples. Average reconstitution exceeded 97%.

All animal experiments were approved by the Swiss Veterinary Office (115/05; Zurich, Switzerland) and performed according to federal and institutional guidelines.

Reagents

Cytokines, growth factors and chemicals were obtained from the following sources. Roche Diagnostics: mTNFα and mIFNγ. PeproTech: rmIL-1b, hIL-2, mIL-6, rmIL-13, rhTGFβ 2, and M-CSF. BD PharMingen: rmIL-10. Antibodies to NG2 were either a kind gift from Prof. William B. Stallcup or obtained from Chemicon. Anti-β-tubulin-HRP and anti-β-actin-HRP were purchased from Abcam and Sigma, respectively. Antibodies to CD3 (biotin), CD4 (PE), CD8 (FITC), CD11b (biotin), B220 (biotin) and Gr1 (FITC), were obtained from BD PharMingen and F4/80 (FITC)

from Serotec. CD11b (unlabelled), CD16/32 (Fc block) and CD45 (APC) were purchased from Biolegend and CD11c (clone N418, PE) from Caltag. The secondary antibody anti-rabbit HRP was obtained from Pierce. Anti-rat Alexa 488 and anti-rabbit Alexa 594 were purchased from Molecular Probes/Invitrogen and Streptavidin-APC-Cy7 Biolegend.

EAE induction

Mice were injected with 100 µg MOG35-55 (Anawa, Switzerland) in 200 µl PBS/CFA (DIFCO, USA) (1:1) subcutaneously on the right flank and with 300 ng Pertussis toxin (List Biological Laboratories, USA) intraperitoneal (i.p.) on day 0, followed by a boost of 300 ng Pertussis Toxin at day 2 and 100 µg MOG35 in CFA into the left flank on day 7. The scoring of clinical symptoms was performed as described previously (Moransard *et al.* , 2010 Apr).

Primary cells and cell lines

Primary oligodendrocyte progenitor cells (OPCs) were isolated as described previously (Moransard *et al.* , 2010 Apr). Briefly, neonatal forebrain cells were harvested from 1-2 day old neonates C57/BL6 mice by dissociation of cortices in Papain (Sigma) and grown in DMEM (Gibco) supplemented with 10% horse serum (HS) (Gibco) on poly-D-lysine (Sigma)-coated cell culture flasks. After 10 days the loosely attached OPCs were separated from the glial feeder layer by 16 h of mechanical shaking at 210 rpm, 37°C. The collected OPCs were further cultured either in SATO medium as described previously (Moransard *et al.* , 2010 Apr) or in DMEM/F12 (Gibco), 10 mom N-Acetyl-L-alary-L-glutamine (L-GLU) (Biochrom AG, Germany), 1% Pen-Strep (Gibco), 2% B-27 supplement (Gibco) on poly-D-lysine coated cell culture flasks.

Bone marrow-derived macrophages (BMM) were prepared from bone marrow cells isolated from the femur and tibia. Bones were flushed with HBSS and the cell suspension was forced through a 70-µm mesh. Collected cells were re-suspended in complete macrophage medium containing DMEM, 30% L929 cell-conditioned medium (source of M-CSF), 20% HS, 10 mom HEPES (Gibco) and 10 mom L-GLU and cultured at 37°C, 5% CO2. After 7 days virtually 100% of the cells expressed the macrophage markers CD11b and F4/80. The cells were harvested by scraping on ice and frozen in 90% FCS and 10% DMSO at a density of 5×10^6-10×10^6 cells/ml. Thawed cells were cultured in either DMEM containing 10% fetal calf serum (FCS) (PAA Laboratories GmbH, Austria), 2 mom L-GLU and 20 mg/ml gentamicin (Sigma) or the same medium without serum.

BV2 cells (lab stock) were cultured in DMEM containing 10% FCS, 2 mom L-GLU and 20 mg/ml gentamicin.

OLIneu cells (kindly provided by Dr. J. Trotter) were cultured as described for primary OPCs.

To determine NG2 expression, all cell types were seeded on 3 cm culture dishes at 1.0-2.0$\times10^6$ cells/dish and treated with cytokines for 48 h prior to real time PCR or Western blot analysis. For immunocytochemistry, cells were grown at similar densities on glass cover slips.

Isolation of CNS-mononuclear cells

CNS-mononuclear cells were isolated as described previously (Moransard *et al.* , 2010 Apr). Briefly, brains and spinal cords of animals perfused with Hanks' balanced salt solution (HBSS) were minced with a scalpel blade and digested for 30’ at 37°C in HBSS containing 50 mg/ml DNase I and 100 mg/ml Collagenase/Dispase (Roche). The digestion was quenched on ice and passed through a 100 µm Nylon mesh (BD

Biosciences) and centrifuged after which the pellet re-suspended in 30% Percoll (Sigma). The gradient was centrifuged at 29000 x g for 30 min at 4°C (Kontron Instruments, Germany). The top layer containing myelin was removed by aspiration, and the interphone containing mononuclear cells was collected, diluted threefold with HBSS and collected by centrifugation at 300 x g.

Flow cytometric analysis

Cells were re-suspended in FACS buffer containing 2% FCS, 5 mom EDTA, 0.01% NaN_3 in phosphate buffered saline (PBS). Prior to staining with the appropriate antibodies, Fc receptors were blocked by incubation with anti mouse CD16/32 (Fc-block, BD PharMingen). 7-Amino-actinomycin D (7-AAD) was used to exclude non-viable cells. All flow cytometric data was obtained with a CyFlow flowcytometer (Partec, Germany). Data analysis was performed with FlowJo.

Infiltrating mononuclear cells were distinguished from CNS-resident microglia ($CD45^{int}/CD11b^{+}/F4/80^{+}$) on the basis of their high CD45 expression. Within this population the following cell types were distinguished using gating as indicated between brackets: CD4 T cells ($CD3^{+}/CD4^{+}$), CD8 T cells ($CD3^{+}/CD8^{+}$), Granulocytes (CD11b+/Gr1+), lyDCs (lymphoid dendritic cells; $CD11c^{+}/CD11b^{-}/F4/80^{-}$), myDCs (myeloid DCs; $CD11c^{+}/CD11b^{+}/F4/80^{-}$), inflDCs (inflammatory DCs; $CD11c^{+}/CD11b^{+}/F4/80^{+}$), pDCs (plasmacytoid DCs; $CD11c^{+}/B220^{+}/Gr1^{+}$), B cells ($CD11c^{-}/B220^{+}/Gr1^{-}$), Macrophages ($CD11c^{-}/CD11b^{+}/F4/80^{+}$).

Western blotting

To determine the amount of cell-bound NG2, cultured cells were scraped on ice in lysis buffer containing 1% Nonidet P 40 (NP-40, Igepal CA 630, Fluka), 50 mom Tris, 150 mom NaCl, 5 mom EDTA and a cocktail of proteinase inhibitors (Complete Mini, Roche), after which the lysates were cleared from insoluble material by

centrifugation. To determine the amount of secreted NG2, cell-conditioned media were collected and concentrated 10 fold using Amicon Ultra centrifugal filter devices with a cut-off of 100 kDa (Amicon). Both lysates and cell conditioned-media were incubated for 3 hrs at 37°C with Chondroitinase ABC (Sigma) in order to remove the chondroitin side chain of NG2 prior to incubation with an appropriate volume of Laemmli buffer at 80°C.

The protocol to isolate soluble and detergent-extractable NG2 fractions from CNS tissue is based upon the methods published by Asher *et al*. (Asher *et al.* , 2005). In brief, spinal cords isolated from EAE diseased mice were homogenized on ice with a douncer in the same buffer as used for cultured cells but omitting NP-40. The resulting lysate was cleared of insoluble material by low-speed centrifugation (3000g, 10 min). The supernatant contains soluble NG2, whereas detergent-extractable NG2 was recovered by re-suspending the pellet in lysis buffer containing 1% NP-40. Finally both lysates were cleared from remaining insoluble material by centrifugation (15000g, 10 min) followed by determination of the protein concentration using a BCA protein assay kit (Pierce) and incubation with an appropriate volume of Laemmli buffer at 80°C.

For Western blotting for NG2 equal amounts of protein were loaded on NuPAGE 3-8% Tris-Acetate gels (Invitrogen). Probing for β-tubulin and/or β-actin was performed to control for loading. Images of Western blots were obtained and quantified using the GE Health care ImageQuant 350 system and accompanying software.

Immunohistochemistry/Immunocytochemistry

Mice were CO_2 anesthetized and perfused with 25 ml Ringer solution (Braun Medical AG, Switzerland). Immunohistochemistry was performed on 10-15 μm frozen, 4%

PFA- or methanol-fixed longitudinal or cross sections of thoracic and lumbar spinal cord. Sections were thawed, fixed and blocked (5% FCS, 0.01% triton, PBS) prior to incubation with primary antibody 1/200 in block buffer for 24 h. After washes with PBS, sections were incubated with the appropriate secondary antibody in block buffer for 2 h. After counterstaining with DAPI (Molecular Probes) sections were mounted in Mowiol embedding medium (Mowiol 4-88, Calbiochem) containing 0.1% 1,4-Diazabicyclo-82.2.29-octan (DABCO, Fluka). Immunocytochemistry on cultured cells was performed using the same protocol directly after a short wash and fixation of the cells with 4% PFA for 10 minutes. Images were obtained on either a Zeiss Axiovert 40 or a Leica SP 5 confocal microscope.

Histology

Mice were sacrificed with CO_2. Histology was performed as described recently (Prinz *et al.* , 2006). Spinal cords were removed and fixed in 4% buffered formalin and embedded in paraffin before staining with hematoxylin eosin (H&E) or luxol fast blue (LFB) to assess the degree of demyelination, MAC-3 (BD PharMingen) for macrophages and microglia, CD3 for T cells (Serotec), B220 (BD PharMingen) for B cells, APP for amyloid precursor protein (Chemicon), and GFAP for astrocytes (Dako).

Electron microscopy and evaluation of remyelination

Electron microscopy and evaluation of remyelination was performed as recently described (Raasch *et al.* , 2011): Epon-embedded, glutaraldehyde-fixed spinal cord slices from lumbar spinal cords (L1-L4) from 5 WT and 5 NG2 animals at d40 p.i. and 4 WT and 3 NG2 age and sex matched healthy control animals were prepared, cut and stained with toluidine blue. This staining allowed clear distinction between normal and inflamed white matter already by light microscopy. The tissue was then

trimmed and re-orientated so that ultrathin cross sections of the spinal cord could be cut and treated with urinal acetate and lead citrate. 30 Electron micrographs from within spinal cord sections were obtained at 13500-fold magnification from each animal. Of these 10 images for each animal were randomly selected and axon diameter and myelin thickness were measured using the analySIS Dock System (Soft Imaging System GmbH, Germany). Within each image all axons with diameters of larger than 250 nm were evaluated, axons with smaller diameters were omitted, since these are usually un-myelinated axons. This meant that at least 130 axons per animal were evaluated. G ratios were defined as diameter of the axon divided by fiber diameter (axon plus myelin). We calculated a G ratio for each fiber and subsequently averaged all G ratios from one spinal cord. In addition, the number of myelinated fibers in relation to all fibers was expressed as percentage of myelinated axons to all visible axons. Electron micrographs were obtained using a Philips CM 100 electron microscope.

RNA isolation and real time PCR

Whole-cell RNA from cultured cells was extracted using the NucleoSpin-RNA II kit (Macherey-Nagel, Switzerland). RNA from mouse tissues was extracted by homogenization in TRIzol (Invitrogen) according to the manufacturer's instructions. RNA was reverse-transcribed using random hexamers and AMV reverse transcriptase (Promega). The cDNA equivalent to 50 ng of total RNA was PCR-amplified in an ABI PRISM 7700 detection system (PE-Applied Biosystems) using TaqMan Universal PCR Master Mix (Applied Biosystems) and quantified using the $2^{-\Delta\Delta CT}$ method using 18s rRNA as a housekeeping gene. Relative RNA levels are expressed as x-fold variations compared to control. Primers and probes for Taqman analysis for

IL-2, IL-6, IL-10, TNFα, IFNγ, TGFβ and NG2 were purchased from Applied Biosystems.

Proliferation assay

OLIneu were seeded in a 96 well plate and treated with cytokines for 16 h before the addition of 5 μCi/ml ^{3}H-thymidine (GE Healthcare). After incubate for 16 h at 37°C the cells were harvested directly onto a glass fiber filter membrane using a 96-well plate harvester. The filters were dried at 60°C, sealed in a plastic bag containing scintillation fluid (PerkinElmer) and measured in a beta-counter (PerkinElmer).

Statistical analysis

For data obtained *in vivo* we performed unpaired, two-tailed Student's t-tests assuming equal variances. For data obtained *in vitro* we performed paired, two-tailed Student's t-tests assuming equal variances. Numbers following the ± sign represent standard error (s.e.m).

Acknowledgements

The authors would like to thank Lara Ogunshola for critical reading of the manuscript. We thank the Center for Microscopy and Image Analysis, Zürich, Switzerland, for their expert help and use of confocal microscopes. This study was supported by the Swiss National Science Foundation and the National Competence Centre (NCCR) Neuronal Plasticity and Repair, Switzerland. A.F. is Hertie Senior Research Professor Neuroscience of the Gemeinnützige Hertie-Stiftung.

Author Contributions

M.M. conceived the study, designed and performed all experiments, analyzed data and wrote the manuscript; A.D. performed and analyzed the histology in figure 3C and D; O.S. is responsible for all the data and analysis presented in figure 4; T.S. generated the chimeric mice, assisted in experiments and commented on the manuscript; M.P. and A.F. gave conceptual advice and commented on the manuscript.

Figure legends

Figure 1. NG2 is up regulated and accumulated in and around areas of leukocyte infiltration at peak and remitting stages of EAE.

(**A**) Quantitative RT-PCR analysis of NG2 and cytokine mRNA expression in spinal cord at different EAE stages. NG2 mRNA expression is significantly increased at peak and remission (rem.). The expression of NG2 mRNA correlates well with TGFβ mRNA expression, but not with the expression of IL-2, IL-6, IL-10, TNFα or IFNγ. (**B, C**) Western blot and corresponding densitometric quantitation of soluble and detergent-extracted NG2 in spinal cord lysates from EAE diseased mice. Both soluble and detergent-extracted NG2 protein amounts are significantly elevated in spinal cord at peak and remission (rem.). (**D**) Immunohistochemistry for NG2 in longitudinal sections of spinal cord. In the spinal cord of naïve animals NG2 expression is confined to blood vessels and oligodendrocyte progenitor cells (OPCs). Insert shows an electronically 3x magnified image of a stellate OPC in the boxed area. At peak and remission, NG2 immunoreactivity is increased in and around areas of infiltrating leukocytes, identified by DAPI staining as clustered nuclei. NG2 immunoreactivity is diffuse and does not resemble the classic OPC morphology. Inserts show electronically 3x-magnified images of the boxed areas. In normal appearing spinal cord at remission (rem. n.a. Sp.C.), NG2 immunoreactivity is not increased and is localized to OPCs and blood vessels. Bars represent mean ± s.e.m., n=4 , *P<0.05, **P<0.01 versus naïve WT control.

Figure 2. TGFβ induces expression and secretion of NG2 by macrophages and OPCs *in vitro*.

(**A**) Analysis of NG2 mRNA expression in (primary bone marrow-derived) macrophages (Mac.) and OLIneu treated with different cytokines (24 hrs) by quantitative RT-PCR. NG2 expression is significantly increased by treatment with TGFβ in OLIneu and macrophages. IL-6 also increases NG2 expression in OLIneu. (**B**) Representative Western blot for NG2 of primary OPC lysates and culture medium after 48 hrs of TGFβ treatment. TGFβ up regulates both cell bound and secreted NG2. (**C, D**) Western blot for NG2 of macrophage lysates and culture medium after cytokine treatment (24 hrs) and corresponding densitometric quantitation. Untreated macrophages express and secrete a small amount of NG2. TGFβ elicited a significant increase in cell-bound and secreted NG2. (**E**) Treatment of the microglia cell line BV2 with cytokines followed by Western blot analysis of cell lysates and culture media. Microglia express cell-bound NG2 only after TGFβ treatment. Secreted NG2 could not be detected. (**F**) Comparative Western blot of NG2 expression in macrophages, microglia (Micr.) and primary OPCs. Macrophages express a modest amount of NG2 although at lower levels than expressed by OPCs. NG2 expressed by microglia is barely detectable. (**G**) Immunocytochemistry for NG2 in OLIneu, macrophages and microglia after cytokine treatment. TGFβ treatment induces an increase in NG2 immunoreactivity in OLIneu. TGFβ elicits NG2 expression in most, but not all, macrophages (co-stained with CD11b). NG2 immunoreactivity is never detected in microglia. Bars represent mean ± s.e.m., n=4, *P<0.05, **P<0.01 versus control.

Figure 3. NG2 deficiency does not alter EAE disease progression or inflammatory profile.

(**A**) EAE progression monitored in mice immunized with MOG using a method that scores the degree of paralysis on a 1 to 5 scale. Shown are the combined results of 2 independent experiments with 24 NG2 deficient (NG2ko) and 36 WT animals in total. (**B**) Progression of weight loss of the same mice. The fluctuations in weight correlate well with the degree of disability. NG2-deficiency has no effect on EAE progression. (**C, D**) Histology and corresponding quantitation of thoracic spinal cord cross sections from EAE diseased NG2ko and WT mice at the remission stage for myelin loss (LFB; luxol fast blue), neuronal damage (APP; amyloid precursor protein), astrocyte proliferation (GFAP; glial fibrillary acidic protein), and infiltration of macrophages (MAC-3) and T-cells (CD3). In addition the number of infiltrating B cells was assessed (B220). No significant differences in the number of infiltrating cells or degree of demyelination or neuronal damage were detected (n=5). (**E**) Flow cytometric analysis of CNS-infiltrating leukocytes. No significant differences were found in any of the leukocyte populations tested. For gating strategy and definition of leukocyte populations see Methods. Bars represent mean ± s.e.m., n=4. (**F**) Immunohistochemistry for macrophages/microglia (CD11b and F4/80) on thoracic spinal cord cross-sections (peak). In WT animals, NG2 accumulation appears associated with infiltrates of CD11b and F4/80 positive macrophages/microglia. The number of infiltrating cells and area occupied does not noticeably differ between WT and NG2ko animals.

Figure 4: Normal myelination and remyelination in the absence of NG2.

(**A**) Spinal cord sections from WT and NG2 animals d40 p.i. and from sex- and age-matched healthy controls. First row: Toluidine Blue stained sections (scale bars = 500 μm), box depicts areas evaluated for myelination. Second row: magnified sections

from first row (scale bars = 100 μm). Third row: Electron micrographs of evaluated regions (scale bars = 1 μm). (**B-E**) Percentage of myelinated axons compared to all visible axons (**B**), average axon diameter (**C**), average myelin thickness (**D**) and average G-Ratio (**E**) show no significant differences between WT and NG2 animals in either the d40 p.i. or the control groups. (P-values >0.1). Animals at d40 p.i. show significantly reduced myelination compared to healthy control animals (*=P<0.05; **=P<0.01). In all the graphs, each data point represents an individual animal. Mean values are also depicted.

Figure 5. CNS resident cells are responsible for increased NG2 expression and accumulation in and around areas of leukocyte infiltration. (**A, B**) EAE progression and weight loss of the different chimeras. WT→WT n=10, KO→WT n=8, WT→KO n=8. The fluctuations in weight correlate well with the degree of disability. EAE progression is comparable in all groups. (**C, D**) Western blot analysis and corresponding densitometric quantitation of NG2 in spinal cord of EAE diseased chimeras at remission. Soluble and detergent-extracted NG2 amounts are elevated in WT→WT and KO→WT chimeras compared to naïve WT controls. NG2 is not detected in WT→KO spinal cord lysates. Increased cell-bound and secreted NG2 protein amounts are comparable between WT→WT and K→WT chimeras. (**E**) Immunohistochemistry for CD11b and NG2 on thoracic spinal cord cross sections from EAE diseased chimeric mice at remission analyzed by confocal microscopy. WT→WT chimeras show extensive NG2 accumulation in and around areas of leukocyte infiltration, which partly overlaps with CD11b immunoreactivity. KO→WT mice show a similar degree of infiltration of $CD11b^+$ cells and a comparable degree of NG2 accumulation. The overlap between CD11b and NG2

staining appears less frequent. WT→KO animals show a comparable infiltration of $CD11b^+$ cells. However, NG2 staining is almost completely absent. Only occasionally $NG2^+$ cells can be detected in the infiltrate (inserts). These cells also express low levels of CD11b (overlay and insert). Arrows indicate CD11b and NG2 co-localization. Inserts show electronically 2.35x-magnified images of the boxed areas. Bars represent mean ± s.e.m., n=4, *P<0.05, ***P<0.001 versus control.

Supplementary Figure 1. TGFβ treatment does not alter OPC proliferation *in vitro*.

Determination of proliferation of OLIneu treated with TGFβ, TNFα, or IFNγ by ^{3}H-thymidine incorporation. 16h treatment of OLIneu with these cytokines did not alter proliferation.

Supplementary Figure 2. TGFβ treatment increases cell-bound and secreted NG2 in OLIneu in a time dependent fashion.

(**A**) TGFβ time-course treatment of OLIneu followed by Western blot analysis for NG2 of cell lysates and culture medium. (**B**) Corresponding densitometric quantitation. Cell-bound and secreted NG2 protein levels are significantly elevated after 24 hrs of TGFβ treatment. Bars represent mean ± s.e.m., n=4, *P<0.05 versus untreated control.

Supplementary Figure 3. $Olig2^+$ OPCs are detected within and around sites of leukocyte infiltration.

Immunohistochemistry for Olig2 in transfer sections of thoracic spinal cord. In the spinal cord of peak EAE mice $Olig2^+$ OPCs are found within (arrow) and in close

proximity (arrow heads) to sites of leukocyte infiltration (identified by a high concentration of DAPI stained nuclei).

References

Alonso G. NG2 proteoglycan-expressing cells of the adult rat brain: possible involvement in the formation of glial scar astrocytes following stab wound. Glia. 2005 Feb;49(3):318-38.

Asher RA, Morgenstern DA, Properzi F, Nishiyama A, Levine JM, Fawcett JW. Two separate metalloproteinase activities are responsible for the shedding and processing of the NG2 proteoglycan in vitro. Mol Cell Neurosci. 2005 May;29(1):82-96.

Bocchini V, Mazzolla R, Barluzzi R, Blasi E, Sick P, Kettenmann H. An immortalized cell line expresses properties of activated microglial cells. J Neurosci Res. 1992 Apr;31(4):616-21.

Bu J, Akhtar N, Nishiyama A. Transient expression of the NG2 proteoglycan by a subpopulation of activated macrophages in an excitotoxic hippocampal lesion. Glia. 2001 Jun;34(4):296-310.

Chen ZJ, Ughrin Y, Levine JM. Inhibition of axon growth by oligodendrocyte precursor cells. Mol Cell Neurosci. 2002 May;20(1):125-39.

Dawson MR, Levine JM, Reynolds R. NG2-expressing cells in the central nervous system: are they oligodendroglial progenitors? J Neurosci Res. 2000 Sep 1;61(5):471-9.

de Castro R, Jr., Tajrishi R, Claros J, Stallcup WB. Differential responses of spinal axons to transection: influence of the NG2 proteoglycan. Exp Neurol. 2005 Apr;192(2):299-309.

Di Bello IC, Dawson MR, Levine JM, Reynolds R. Generation of oligodendroglial progenitors in acute inflammatory demyelinating lesions of the rat brain stem is associated with demyelination rather than inflammation. J Neurocytol. 1999 Apr-May;28(4-5):365-81.

Dou CL, Levine JM. Inhibition of neurite growth by the NG2 chondroitin sulfate proteoglycan. J Neurosci. 1994 Dec;14(12):7616-28.

Fawcett JW, Asher RA. The glial scar and central nervous system repair. Brain Res Bull. 1999 Aug;49(6):377-91.

Fiedorowicz A, Figiel I, Zaremba M, Dzwonek K, Oderfeld-Nowak B. The ameboid phenotype of NG2 (+) cells in the region of apoptotic dentate granule neurons in trimethyltin intoxicated mice shares antigen properties with microglia/macrophages. Glia. 2008 Jan 15;56(2):209-22.

Foote AK, Blakemore WF. Inflammation stimulates remyelination in areas of chronic demyelination. Brain. 2005 Mar;128(Pt 3):528-39.

Gao Q, Lu J, Huo Y, Baby N, Ling EA, Dheen ST. NG2, a member of chondroitin sulfate proteoglycans family mediates the inflammatory response of activated microglia. Neuroscience. 2010 Jan 20;165(2):386-94.

Grako KA, Ochiya T, Barritt D, Nishiyama A, Stallcup WB. PDGF (alpha)-receptor is unresponsive to PDGF-AA in aortic smooth muscle cells from the NG2 knockout mouse. J Cell Sci. 1999 Mar;112 (Pt 6):905-15.

Hampton DW, Rhodes KE, Zhao C, Franklin RJ, Fawcett JW. The responses of oligodendrocyte precursor cells, astrocytes and microglia to a cortical stab injury, in the brain. Neuroscience. 2004;127(4):813-20.

Hesske L, Vincenzetti C, Heikenwalder M, Prinz M, Reith W, Fontana A, et al. Induction of inhibitory CNS-derived and stimulatory blood-derived DCs suggests a dual role for GM-CSF in CNS inflammation. Brain. 2010 Jun;133(6):1637-54.
Hossain-Ibrahim MK, Rezajooi K, Stallcup WB, Lieberman AR, Anderson PN. Analysis of axonal regeneration in the central and peripheral nervous systems of the NG2-deficient mouse. BMC Neurosci. 2007 Sep 27;8:80.
Jones LL, Yamaguchi Y, Stallcup WB, Tuszynski MH. NG2 is a major chondroitin sulfate proteoglycan produced after spinal cord injury and is expressed by macrophages and oligodendrocyte progenitors. J Neurosci. 2002 Apr 1;22(7):2792-803.
Kucharova K, Stallcup WB. The NG2 proteoglycan promotes oligodendrocyte progenitor proliferation and developmental myelination. Neuroscience. 2010 Mar 10 Dec 16;166(1):185-94.
Laabs TL, Wang H, Katagiri Y, McCann T, Fawcett JW, Geller HM. Inhibiting glycosaminoglycan chain polymerization decreases the inhibitory activity of astrocyte-derived chondroitin sulfate proteoglycans. J Neurosci. 2007 Dec 26;27(52):14494-501.
Larsen PH, Wells JE, Stallcup WB, Opdenakker G, Yong VW. Matrix metalloproteinase-9 facilitates remyelination in part by processing the inhibitory NG2 proteoglycan. J Neurosci. 2003 Dec 3;23(35):11127-35.
Levine JM. Increased expression of the NG2 chondroitin-sulfate proteoglycan after brain injury. J Neurosci. 1994 Aug;14(8):4716-30.
Matsumoto H, Kumon Y, Watanabe H, Ohnishi T, Shudou M, Chuai M, et al. Accumulation of macrophage-like cells expressing NG2 proteoglycan and Iba1 in ischemic core of rat brain after transient middle cerebral artery occlusion. J Cereb Blood Flow Metab. 2008 Jan;28(1):149-63.
McKinnon RD, Piras G, Ida JA, Jr., Dubois-Dalcq M. A role for TGF-beta in oligodendrocyte differentiation. J Cell Biol. 1993 Jun;121(6):1397-407.
Mildner A, Mack M, Schmidt H, Bruck W, Djukic M, Zabel MD, et al. CCR2+Ly-6Chi monocytes are crucial for the effector phase of autoimmunity in the central nervous system. Brain. 2009 Sep;132(Pt 9):2487-500.
Moon LD, Fawcett JW. Reduction in CNS scar formation without concomitant increase in axon regeneration following treatment of adult rat brain with a combination of antibodies to TGFbeta1 and beta2. Eur J Neurosci. 2001 Nov;14(10):1667-77.
Moransard M, Sawitzky M, Fontana A, Suter T. Expression of the HGF receptor c-met by macrophages in experimental autoimmune encephalomyelitis. Glia. 2010 Apr Nov 25;58(5):559-71.
Morgenstern DA, Asher RA, Fawcett JW. Chondroitin sulphate proteoglycans in the CNS injury response. Prog Brain Res. 2002;137:313-32.
Nishiyama A, Lin XH, Stallcup WB. Generation of truncated forms of the NG2 proteoglycan by cell surface proteolysis. Mol Biol Cell. 1995 Dec;6(12):1819-32.
Nishiyama A, Yu M, Drazba JA, Tuohy VK. Normal and reactive NG2+ glial cells are distinct from resting and activated microglia. J Neurosci Res. 1997 May 15;48(4):299-312.
Nishiyama A, Komitova M, Suzuki R, Zhu X. Polydendrocytes (NG2 cells): multifunctional cells with lineage plasticity. Nat Rev Neurosci. 2009 Jan;10(1):9-22.

Paglinawan R, Malipiero U, Schlapbach R, Frei K, Reith W, Fontana A. TGFbeta directs gene expression of activated microglia to an anti-inflammatory phenotype strongly focusing on chemokine genes and cell migratory genes. Glia. 2003 Dec;44(3):219-31.
Prinz M, Garbe F, Schmidt H, Mildner A, Gutcher I, Wolter K, et al. Innate immunity mediated by TLR9 modulates pathogenicity in an animal model of multiple sclerosis. J Clin Invest. 2006 Feb;116(2):456-64.
Raasch J, Zeller N, van Loo G, Merkler D, Mildner A, Erny D, et al. I{kappa}B kinase 2 determines oligodendrocyte loss by non-cell-autonomous activation of NF-{kappa}B in the central nervous system. Brain. 2011 Feb 10.
Reynolds R, Dawson M, Papadopoulos D, Polito A, Di Bello IC, Pham-Dinh D, et al. The response of NG2-expressing oligodendrocyte progenitors to demyelination in MOG-EAE and MS. J Neurocytol. 2002 Jul-Aug;31(6-7):523-36.
Rezajooi K, Pavlides M, Winterbottom J, Stallcup WB, Hamlyn PJ, Lieberman AR, et al. NG2 proteoglycan expression in the peripheral nervous system: upregulation following injury and comparison with CNS lesions. Mol Cell Neurosci. 2004 Apr;25(4):572-84.
Rhodes KE, Raivich G, Fawcett JW. The injury response of oligodendrocyte precursor cells is induced by platelets, macrophages and inflammation-associated cytokines. Neuroscience. 2006 Jun 19;140(1):87-100.
Smirkin A, Matsumoto H, Takahashi H, Inoue A, Tagawa M, Ohue S, et al. Iba1(+)/NG2(+) macrophage-like cells expressing a variety of neuroprotective factors ameliorate ischemic damage of the brain. J Cereb Blood Flow Metab. 2009 Mar Oct 28;30(3):603-15.
Stallcup WB. The NG2 proteoglycan: past insights and future prospects. J Neurocytol. 2002 Jul-Aug;31(6-7):423-35.
Tan AM, Zhang W, Levine JM. NG2: a component of the glial scar that inhibits axon growth. J Anat. 2005 Dec;207(6):717-25.
Tan AM, Colletti M, Rorai AT, Skene JH, Levine JM. Antibodies against the NG2 proteoglycan promote the regeneration of sensory axons within the dorsal columns of the spinal cord. J Neurosci. 2006 May 3;26(18):4729-39.
Tang X, Davies JE, Davies SJ. Changes in distribution, cell associations, and protein expression levels of NG2, neurocan, phosphacan, brevican, versican V2, and tenascin-C during acute to chronic maturation of spinal cord scar tissue. J Neurosci Res. 2003 Feb 1;71(3):427-44.
Tigges U, Hyer EG, Scharf J, Stallcup WB. FGF2-dependent neovascularization of subcutaneous Matrigel plugs is initiated by bone marrow-derived pericytes and macrophages. Development. 2008 Feb;135(3):523-32.
Trotter J, Karram K, Nishiyama A. NG2 cells: Properties, progeny and origin. Brain Res Rev. 2010 May Jan 4;63(1-2):72-82.
Ughrin YM, Chen ZJ, Levine JM. Multiple regions of the NG2 proteoglycan inhibit neurite growth and induce growth cone collapse. J Neurosci. 2003 Jan 1;23(1):175-86.
Wu J, Yoo S, Wilcock D, Lytle JM, Leung PY, Colton CA, et al. Interaction of NG2(+) glial progenitors and microglia/macrophages from the injured spinal cord. Glia. 2010 Mar;58(4):410-22.
Yokoyama A, Sakamoto A, Kameda K, Imai Y, Tanaka J. NG2 proteoglycan-expressing microglia as multipotent neural progenitors in normal and pathologic brains. Glia. 2006 May;53(7):754-68.

Zhu L, Lu J, Tay SS, Jiang H, He BP. Induced NG2 expressing microglia in the facial motor nucleus after facial nerve axotomy. Neuroscience. 2010 Mar 31 Jan 6;166(3):842-51.

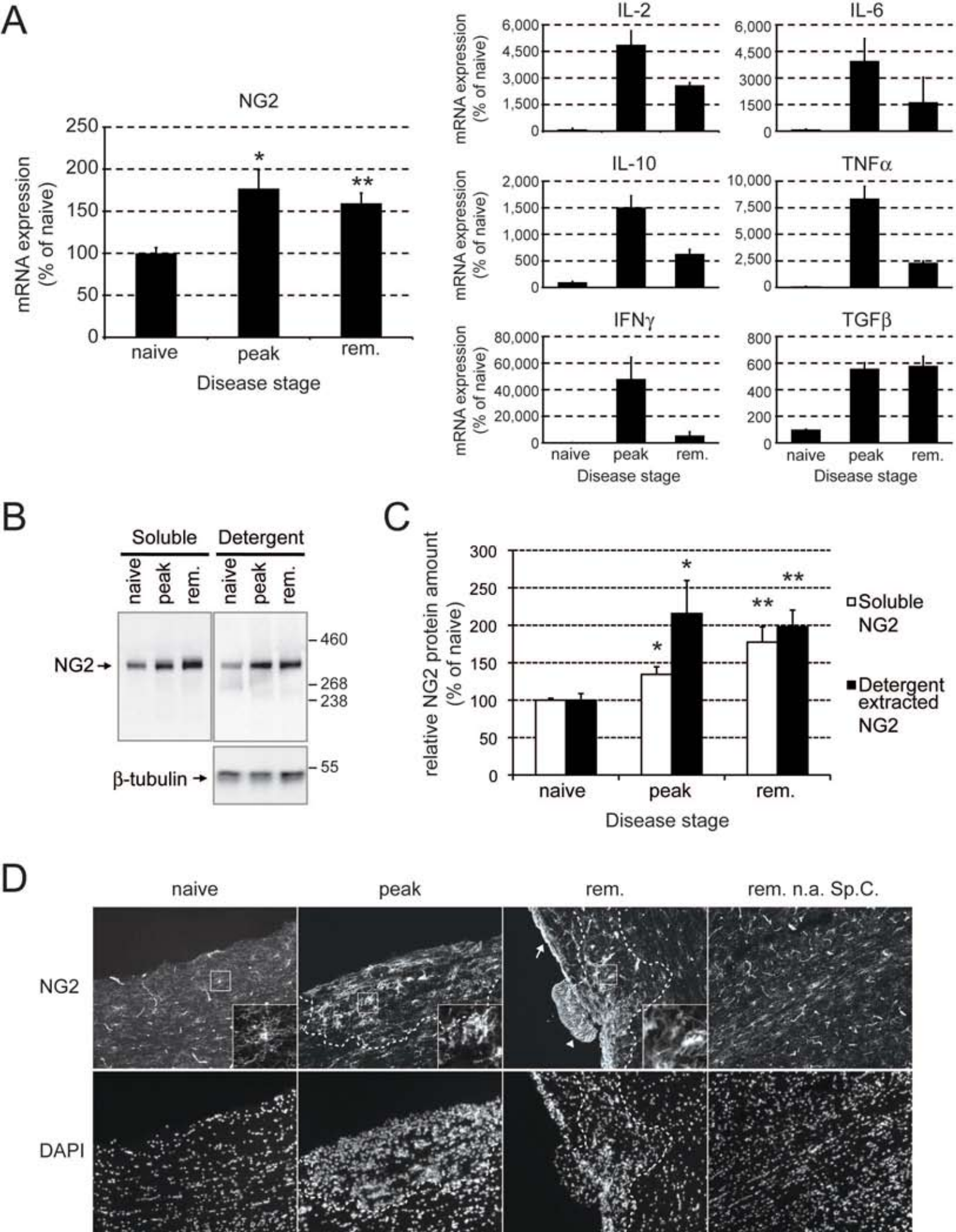
A
NG2
mRNA expression (% of naive)
250
200
150
100
50
0
*
**
naive
peak
rem.
Disease stage
IL-2
IL-6
IL-10
TNFα
IFNγ
TGFβ
6,000
4,500
3,000
1,500
0
2,000
1,000
500
10,000
7,500
5,000
2,500
80,000
60,000
40,000
20,000
800
600
400
200
B
Soluble
Detergent
naive
peak
rem.
NG2
460
268
238
β-tubulin
55
C
relative NG2 protein amount (% of naive)
300
250
200
150
100
50
0
Soluble NG2
Detergent extracted NG2
D
naive
peak
rem.
rem. n.a. Sp.C.
NG2
DAPI

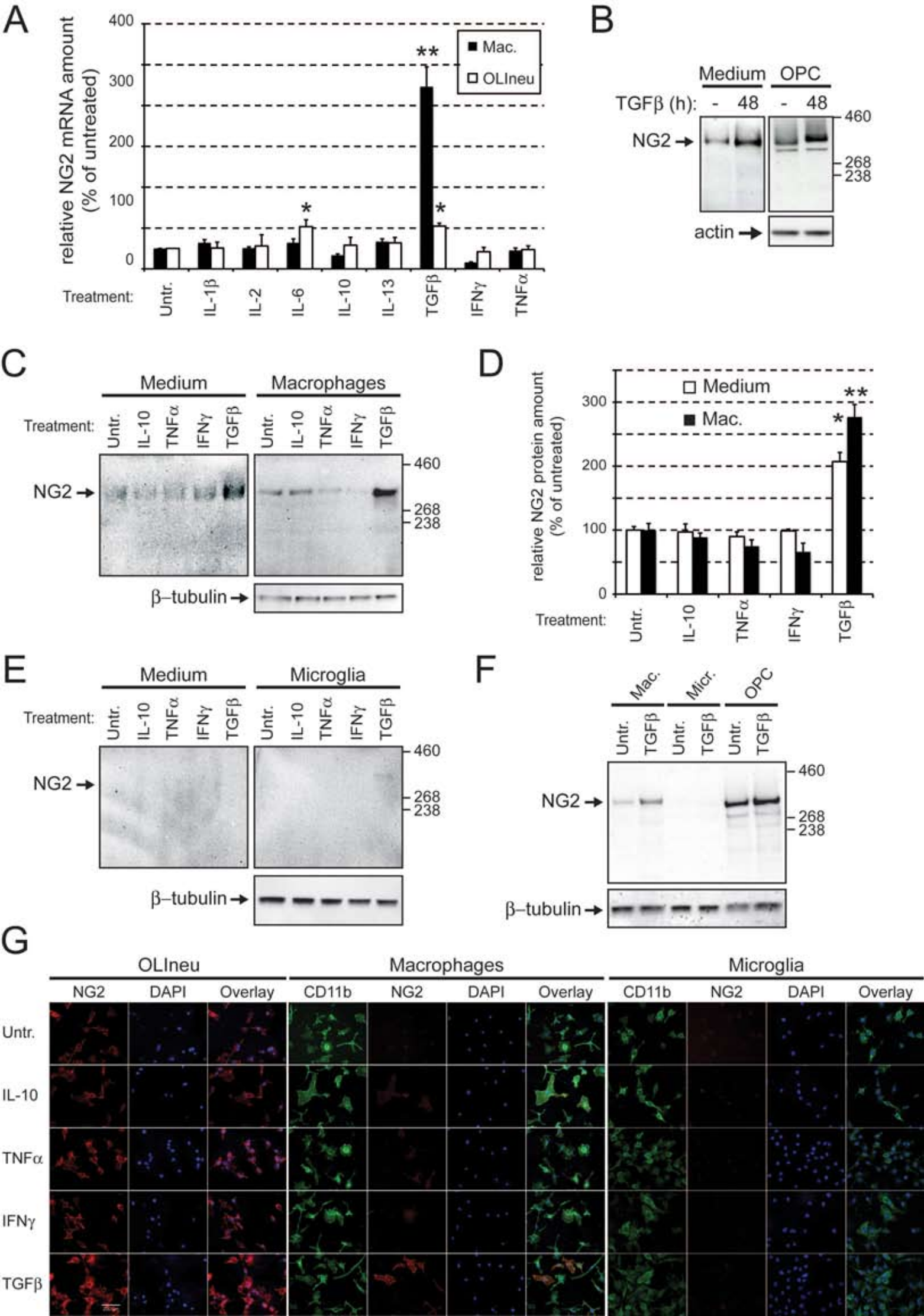
A
relative NG2 mRNA amount (% of untreated)
400
300
200
100
0
Mac.
OLIneu
**
*
*
Treatment:
Untr.
IL-1β
IL-2
IL-6
IL-10
IL-13
TGFβ
IFNγ
TNFα
B
Medium
OPC
TGFβ (h):
-
48
-
48
460
NG2
268
238
actin
C
Medium
Macrophages
Treatment:
Untr.
IL-10
TNFα
IFNγ
TGFβ
NG2
460
268
238
β–tubulin
D
relative NG2 protein amount (% of untreated)
Medium
Mac.
300
200
100
0
*
**
Treatment:
Untr.
IL-10
TNFα
IFNγ
TGFβ
E
Medium
Microglia
Treatment:
Untr.
IL-10
TNFα
IFNγ
TGFβ
NG2
460
268
238
β–tubulin
F
Mac.
Micr.
OPC
Untr.
TGFβ
NG2
460
268
238
β–tubulin
G
OLIneu
Macrophages
Microglia
NG2
DAPI
Overlay
CD11b
Untr.
IL-10
TNFα
IFNγ
TGFβ

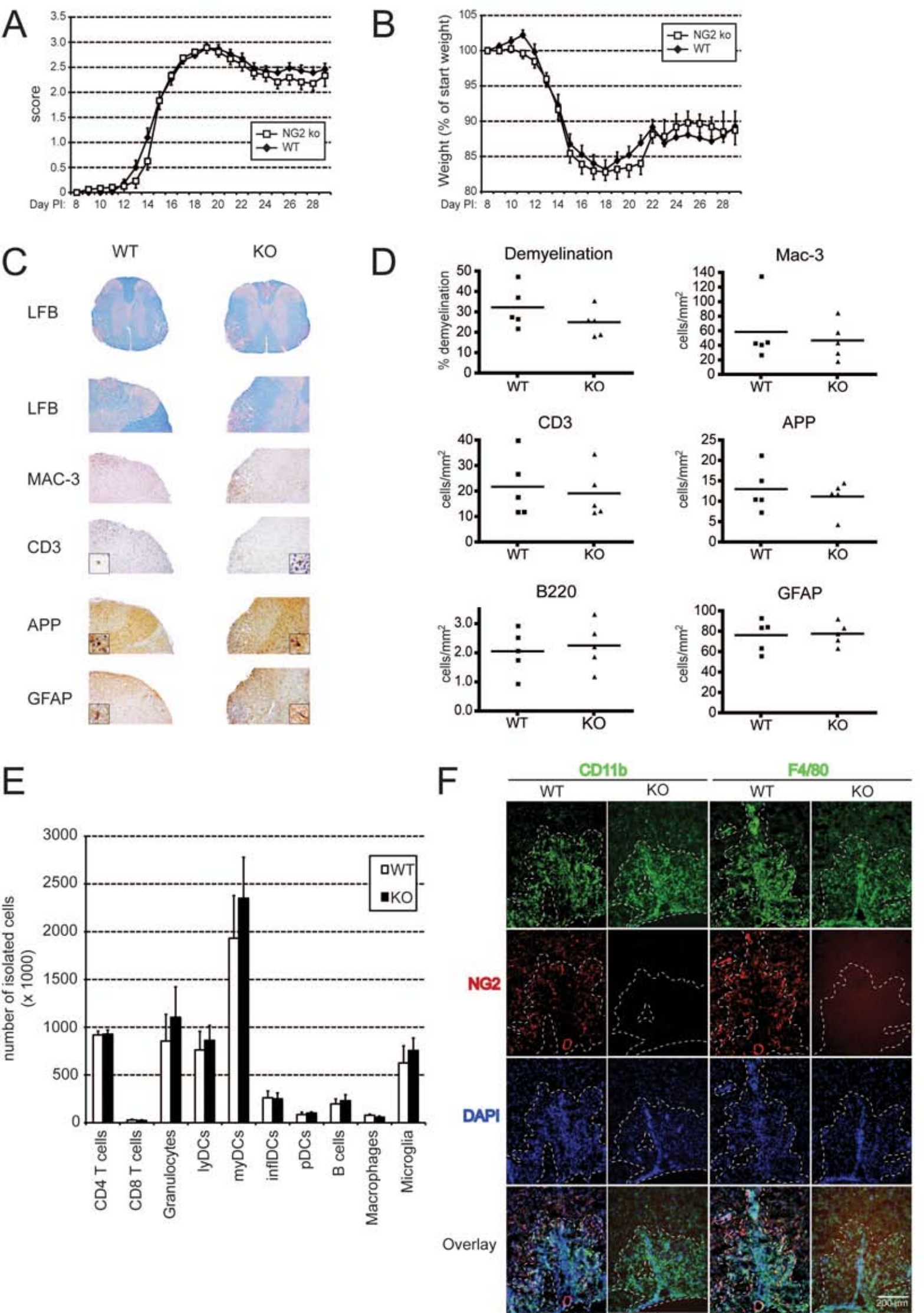
A
score
Day PI: 8 10 12 14 16 18 20 22 24 26 28
NG2 ko
WT
B
Weight (% of start weight)
Day PI: 8 10 12 14 16 18 20 22 24 26 28
NG2 ko
WT
C
WT
KO
LFB
LFB
MAC-3
CD3
APP
GFAP
D
Demyelination
% demyelination
Mac-3
cells/mm2
CD3
cells/mm2
APP
cells/mm2
B220
cells/mm2
GFAP
cells/mm2
WT
KO
E
number of isolated cells (x 1000)
WT
KO
CD4 T cells
CD8 T cells
Granulocytes
lyDCs
myDCs
inflDCs
pDCs
B cells
Macrophages
Microglia
F
CD11b
F4/80
WT
KO
WT
KO
NG2
DAPI
Overlay
200µm

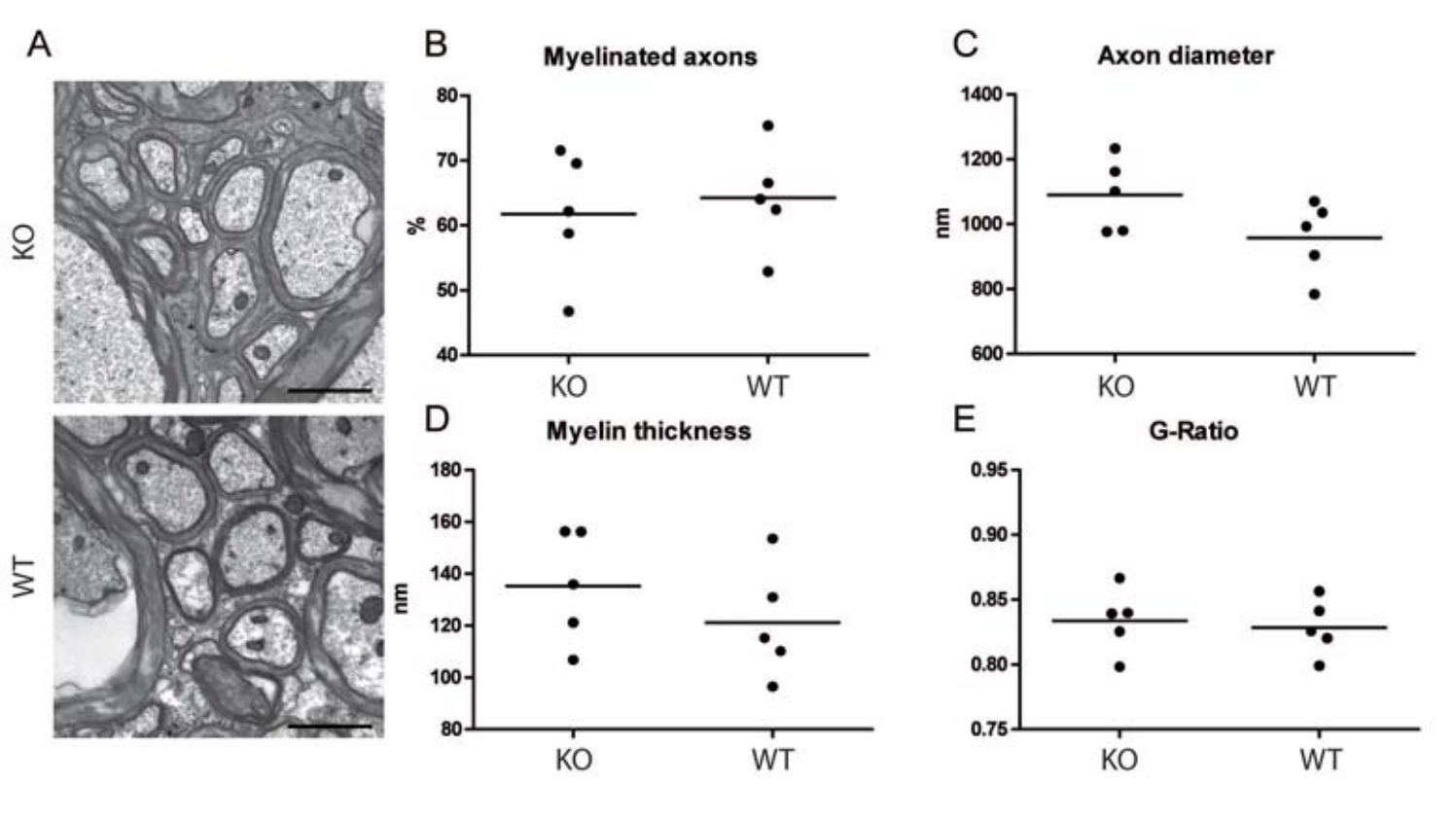
A
KO
WT
B
Myelinated axons
%
80
70
60
50
40
KO
WT
C
Axon diameter
nm
1400
1200
1000
800
600
KO
WT
D
Myelin thickness
nm
180
160
140
120
100
80
KO
WT
E
G-Ratio
0.95
0.90
0.85
0.80
0.75
KO
WT

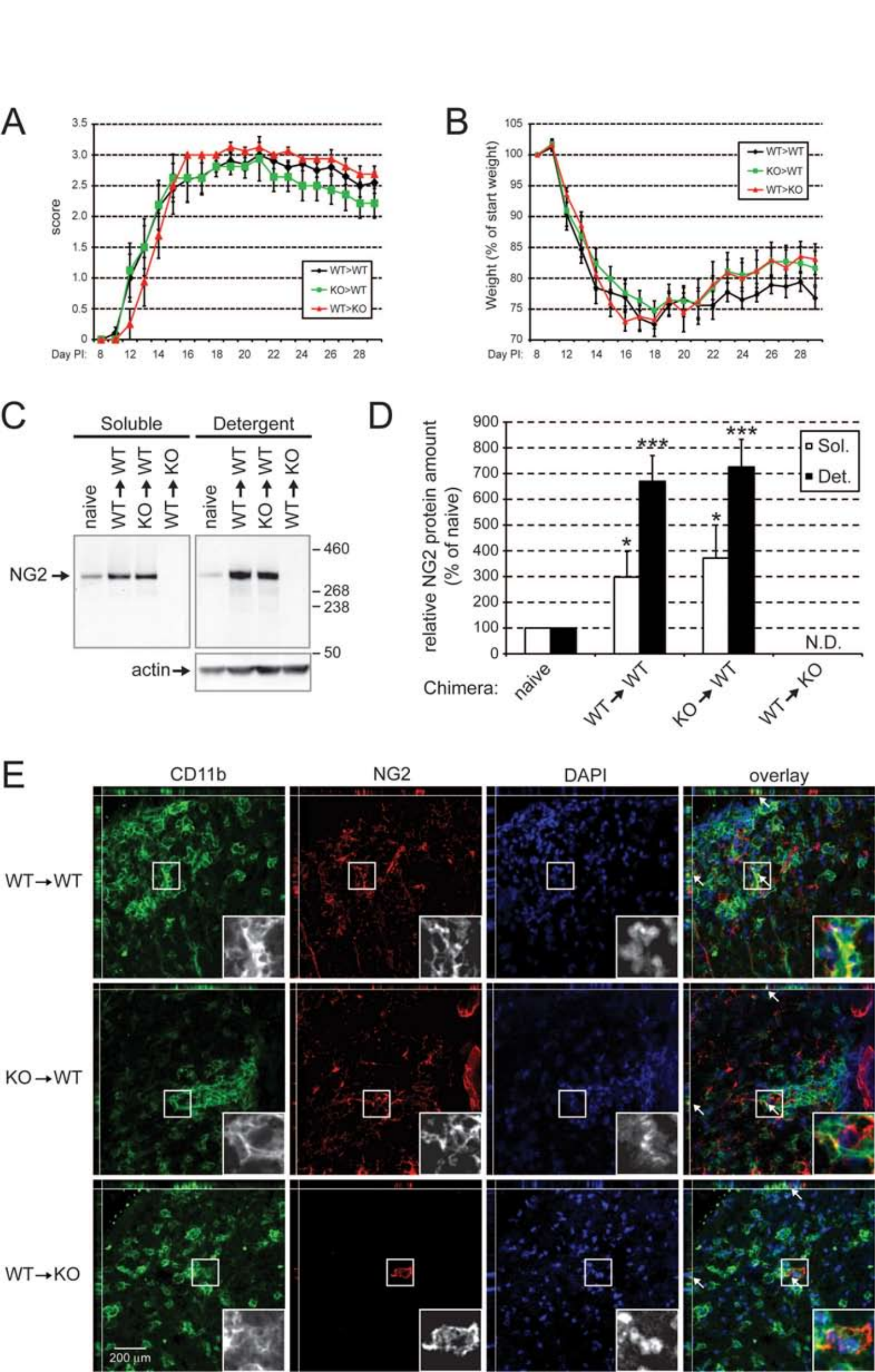
A
score
Day PI:
WT>WT
KO>WT
WT>KO
B
Weight (% of start weight)
Day PI:
WT>WT
KO>WT
WT>KO
C
Soluble
Detergent
naive
WT→WT
KO→WT
WT→KO
NG2
actin
460
268
238
50
D
relative NG2 protein amount (% of naive)
Sol.
Det.
N.D.
Chimera:
naive
WT→WT
KO→WT
WT→KO
E
CD11b
NG2
DAPI
overlay
WT→WT
KO→WT
WT→KO
200 µm

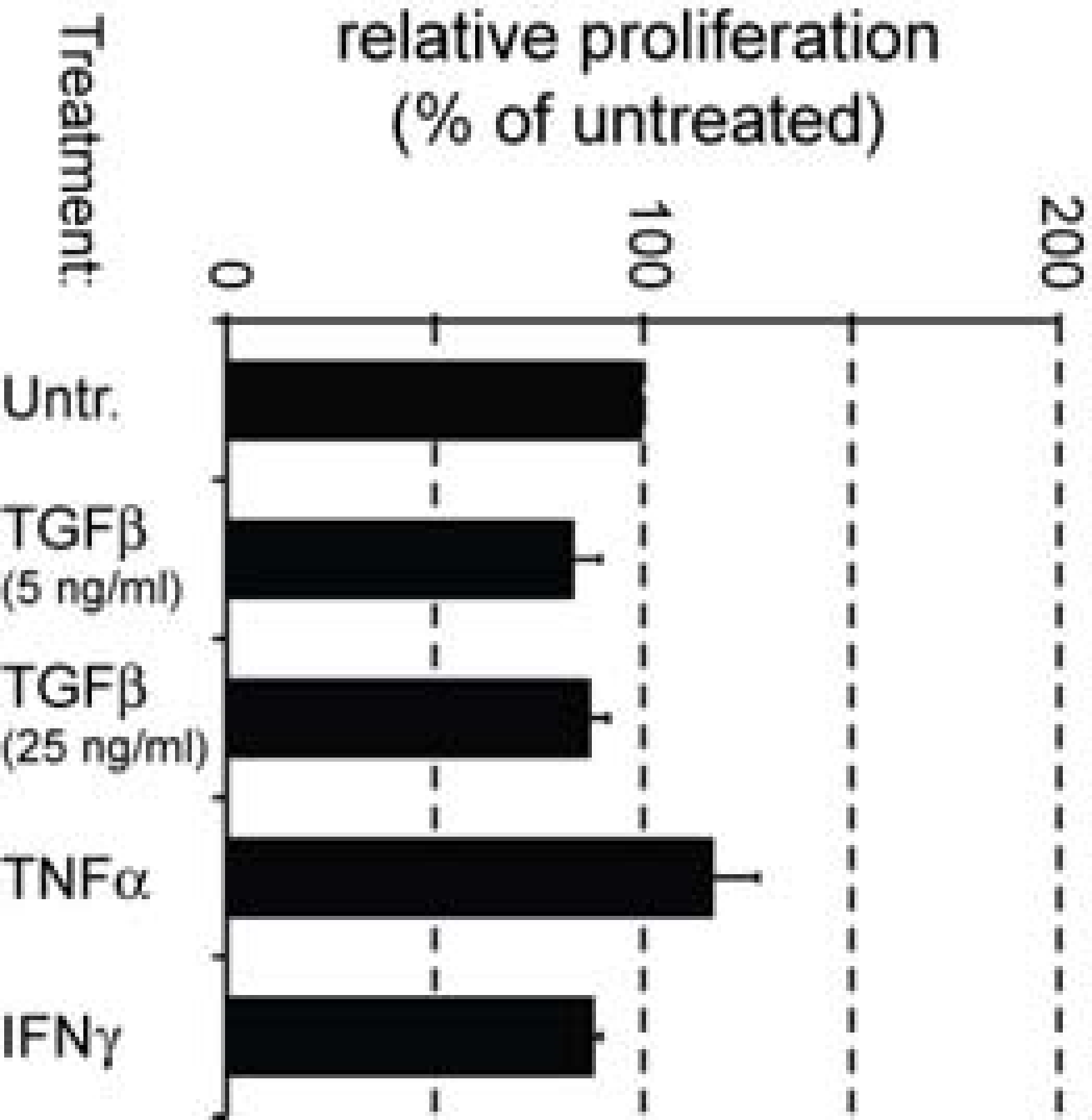
relative proliferation
(% of untreated)
Treatment
0
100
200
Untr.
TGFβ
(5 ng/ml)
TGFβ
(25 ng/ml)
TNFα
IFNγ

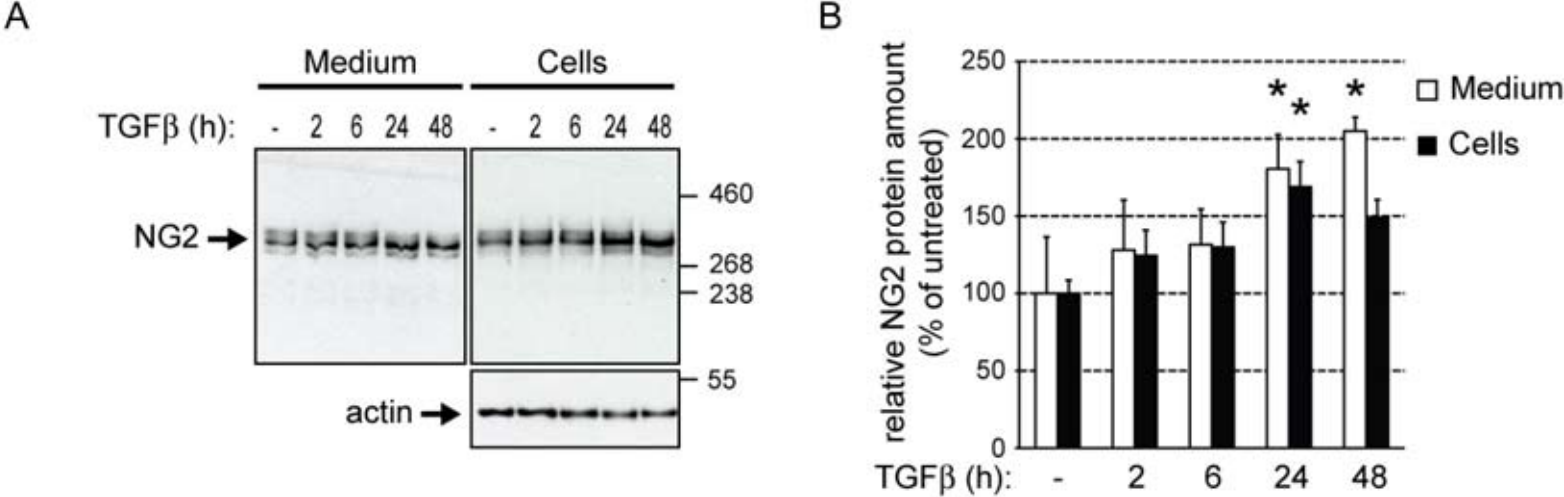
A
Medium
Cells
TGFβ (h):
-
2
6
24
48
-
2
6
24
48
NG2
460
268
238
55
actin
B
relative NG2 protein amount
(% of untreated)
250
200
150
100
50
0
Medium
Cells
*
*
*
TGFβ (h):
-
2
6
24
48

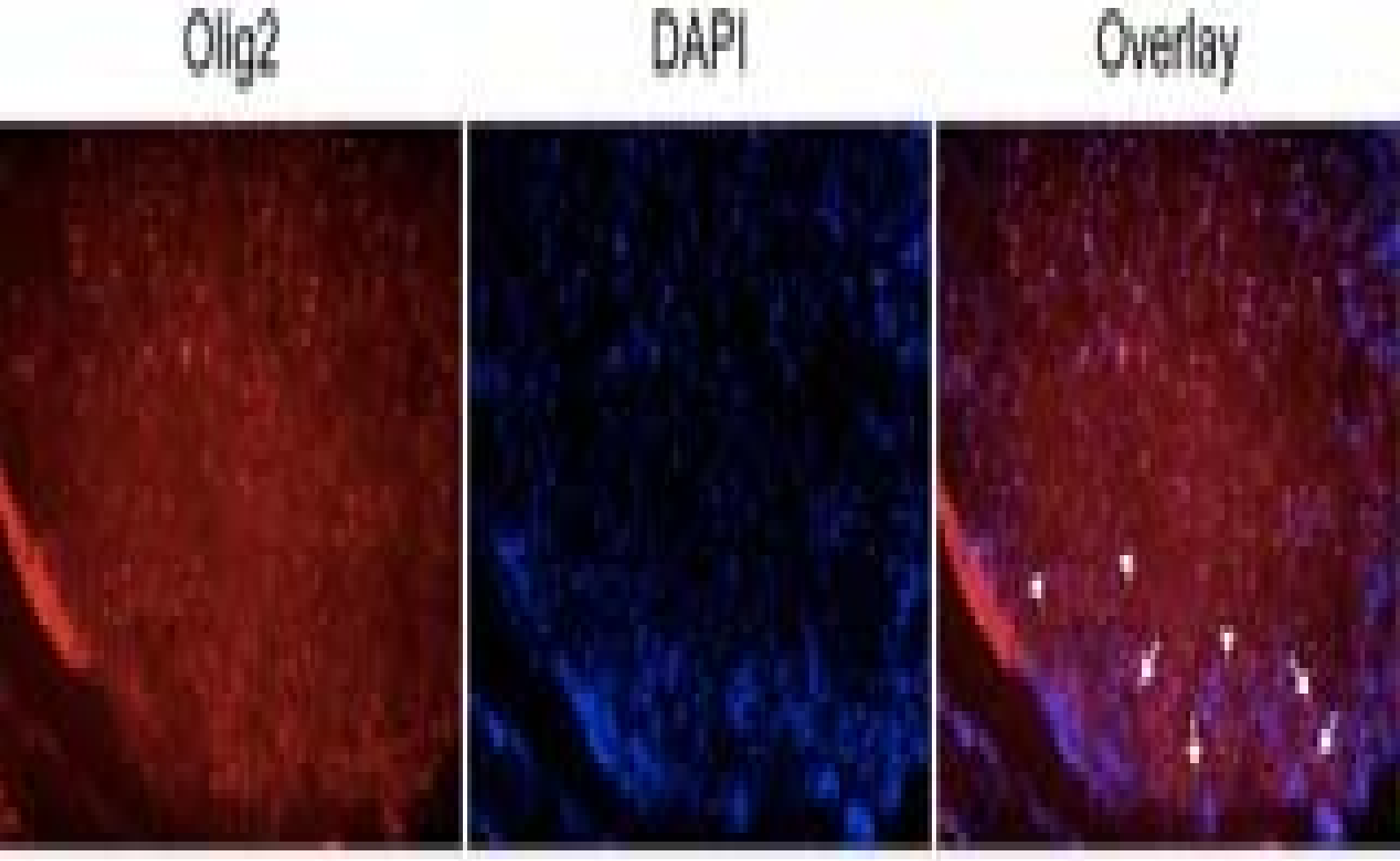
Olig2
DAPI
Overlay